

Direct observation of rupture propagation during the 2011 off the Pacific coast of Tohoku Earthquake (M_w 9.0) using a small seismic array

Hisashi Nakahara¹, Haruo Sato¹, Takeshi Nishimura¹, and Hiroyuki Fujiwara²

¹Department of Geophysics, Graduate School of Science, Tohoku University, Sendai 980-8578, Japan

²National Research Institute for Earth Science and Disaster Prevention, Tsukuba 305-0006, Japan

(Received April 25, 2011; Revised May 31, 2011; Accepted June 2, 2011; Online published September 27, 2011)

A great earthquake of M_w 9.0 occurred on March 11, 2011 off the coast of Tohoku region, Northeast Honshu, Japan. Strong ground motions from the earthquake were recorded at 4 stations of a small seismic array, with an aperture of about 500 m, located 120 km away from the epicenter. Peak ground acceleration exceeded the full scale of $2g$ on the horizontal components, and was larger than $1g$ even on the vertical component. Two prominent bursts and at least two following smaller bursts are identified on the strong-motion records which lasted for longer than 200 s. We have performed semblance analysis to estimate the rupture propagation during the earthquake using coherent seismograms at frequencies of 0.5–2 Hz. The rupture seems to consist of at least four stages. Rupture propagated in a northerly direction in the beginning 50 s forming the first burst, then proceeded to the southwest from the epicenter in the next 50 s during the second burst. The rupture further extended southwest in the following 40 s, and finally migrated to the south for about 30 s. A small seismic array makes it possible to observe rupture propagation during a large earthquake even with a small number of stations.

Key words: The 2011 off the Pacific coast of Tohoku Earthquake, rupture propagation, array, semblance.

1. Introduction

On March 11, 2011, the 2011 off the Pacific coast of Tohoku Earthquake of M_w 9.0 (hereafter called the Tohoku-Oki earthquake) took place at a depth of about 24 km on the plate boundary where the Pacific plate subducts westward beneath the North American plate. The epicenter determined by the Japan Meteorological Agency (JMA) was located at 38.103°N and 142.861°E as shown by a solid star in Fig. 1(a). A thrust-type fault model composed of two subfaults was proposed to explain the observed geodetic data by the Geospatial Information Authority of Japan (GSI) (GSI, 2011) as shown by thick solid rectangles in Fig. 1(a). The average slip of the model is 27.7 m and 5.9 m on the northern and southern subfaults, respectively. The earthquake caused severe ground motions with the largest intensity of 7 on the JMA scale as well as large tsunamis exceeding 10 m in height. Casualties and missing persons exceeding twenty thousand were reported as of the end of March, 2011. However, the full extent of the disaster is not yet clear.

Off the coast of Miyagi prefecture, so-called Miyagi-Ken-Oki earthquakes, having almost the same magnitude (M) of about 7.5, have repeatedly occurred during the last two centuries with the last event taking place on June 12, 1978. The likely source regions of expected earthquakes are identified as three regions (two ellipses and a rectangle) enclosed by thin dotted curves in Fig. 1(a) (the Headquar-

ters for Earthquake Research Promotion (HERP), 2005). In order to record strong ground motions from expected earthquakes, we have been operating, since April, 2004, a small seismic array (hereafter called the Oshika array) comprising 7 strong-motion seismographs with an aperture of about 500 m at the tip of the Oshika peninsula (shown by a solid triangle in Fig. 1(a)).

The Tohoku-Oki earthquake is by far larger than expected earthquakes. Strong ground motions were recorded at 4 stations (solid triangles in Fig. 1(b)) in the Oshika array, which is located about 120 km to the west-north-west of the epicenter. Taking advantage of the small seismic array, we were able to track rupture propagation by a phased array analysis (e.g. Spudich and Cranswick, 1984; Goldstein and Archuleta, 1991; Ishii *et al.*, 2005; Honda *et al.*, 2008). In this paper, we report preliminary results of the array analysis, and provide direct evidence for the rupture propagation during the earthquake.

2. Strong-Motion Data at the Oshika Array

At each station of the Oshika array, a strong-motion instrument, the Kinometrics Altus-K2, is installed on a concrete base. The Altus-K2 has an analogue-to-digital converter with a resolution of 24 bits and a flat frequency response between DC to 40 Hz. The site is located in a pasture. Though the geological structure of the site is identified as a volcanic rock in Mesozoic (early Cretaceous andesite and dacite tuff-breccia and tuff) (Editorial Committee of the Geologic Atlas of Japan, 1992), the shallow structure is not known since no geotechnical or geophysical logging and borehole investigations have yet been undertaken. For more details, we refer to Nakahara *et al.* (2006).

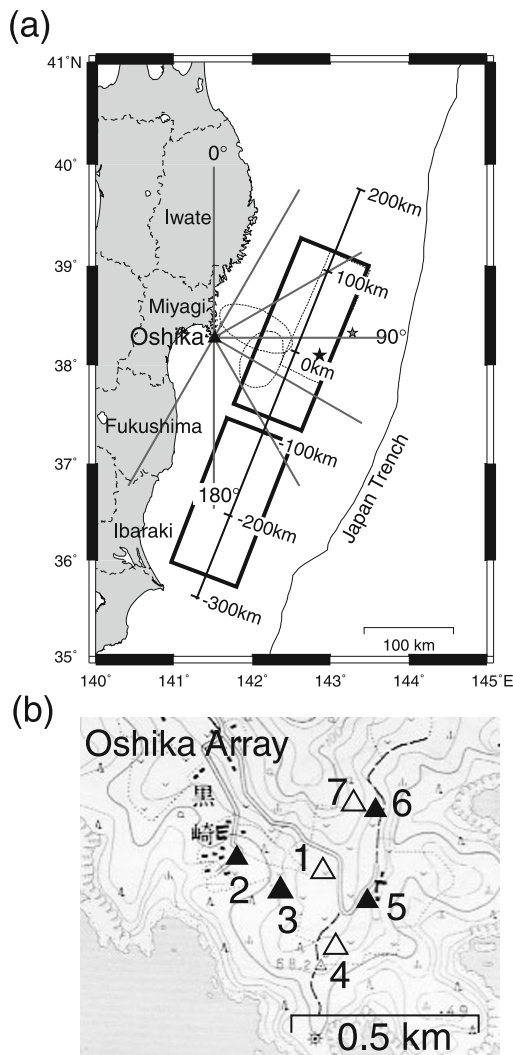


Fig. 1. (a) The location of the Oshika array (solid triangle) and the epicenter of the Tohoku-Oki earthquake (solid star). The gray star is the epicenter of the 9 March, 2011, earthquake. The Japan Trench is shown by a solid curve. The two rectangles drawn with thick solid lines are two subfaults proposed from geodetic observations by GSI. The three regions enclosed by thin dotted curves are the candidate source regions of the expected Miyagi-Ken-Oki earthquake by HERP. Back-azimuths from the Oshika array are shown by radial lines. A linear fault with a strike of 202° is assumed and shown by a thick line, beside which distances are written. The reference point from which the distance is measured is located at 38.145°N and 142.544°E . (b) Configuration of the Oshika array. This map is overwritten on the enlarged 1:25,000-scale topographical map of 'Kinkasan' issued by GSI. There are seven stations constituting the array. A number is attached to each station as shown on the map. Stations with solid triangles were operational at the time of the Tohoku-Oki earthquake.

Strong ground motions from the Tohoku-Oki earthquake were recorded at four stations of the Oshika array with a sampling rate of 100 Hz. The other three stations (shown by open triangles in Fig. 1(b)) were not working due to a malfunctioning of the instruments. In Fig. 2, we show acceleration records for 220 s on east-west (EW), north-south (NS), and vertical (UD) components observed at station OSK2, which is located at 38.27708°N , 141.51656°E , and an elevation of 46 m. Time of 0 s on the records is 14:46:24 on March 11, 2011 (Japan Standard Time (JST) = Universal Time + 9 hours). The earthquake origin time was esti-

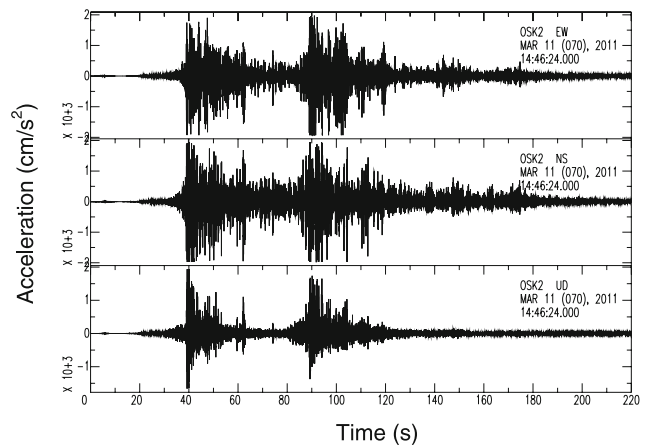


Fig. 2. Acceleration records 220 s long on the EW, NS, and UD components at station OSK2 are shown from top to bottom. Eastward, northward and upward motions are positive. Time of 0 s on the records is 14:46:24 on March 11, 2011 (JST).

mated to be 14:46:18.12 JST by JMA. *P*-wave and *S*-wave onsets are at about 15 s and 30 s on the record, respectively. Large-amplitude motions continued for as long as 200 s after the *S*-wave onset. Two prominent bursts are found at about 40 s and 90 s with durations of a few tens of seconds. At least two additional small bursts are also identified at 140 s and 170 s. Peak ground acceleration (PGA) is large enough to exceed the full scale of 2*g* (*g* denotes the gravitational acceleration) on the horizontal components. Even the UD component shows a PGA larger than 1*g*.

3. Semblance Analysis for Estimating Rupture Propagation

The configuration of the four stations form a quadrangle. Absolute time was maintained by the Global Positioning System. Coherence of seismograms for any pair of stations in the array is known to be high for the frequencies lower than about 2.5 Hz (Nakahara *et al.*, 2006). Therefore we can perform a seismic array analysis to estimate rupture propagation during the earthquake at frequencies lower than about 2.5 Hz. Such a study requires a small seismic array with station separations smaller than a quarter of wavelength studied, because waveform coherence is used. As a measure of the waveform coherence, we use semblance (Neidell and Taner, 1971). Maximizing semblance, we can estimate back-azimuth and horizontal slowness, which is the reciprocal of apparent velocity and is related to incident angle, of the incident phases.

For the calculation of semblance, a frequency band of 0.5–2 Hz is selected. The upper frequency is limited due to the waveform coherence. The lower frequency limit is partly restricted by the signal-to-noise ratio, and this is high down to about 0.05 Hz for the Tohoku-Oki earthquake. In order to track the rupture propagation, however, we need to use high-frequency waves, because they are theoretically considered to be generated at the rupture front due to its acceleration or deceleration (e.g. Madariaga, 1977). It is not easy to define the high frequency objectively. Here, we use a frequency band higher than 0.5 Hz. Even if we change the lower limit to be between 0.1 Hz and 1 Hz, the

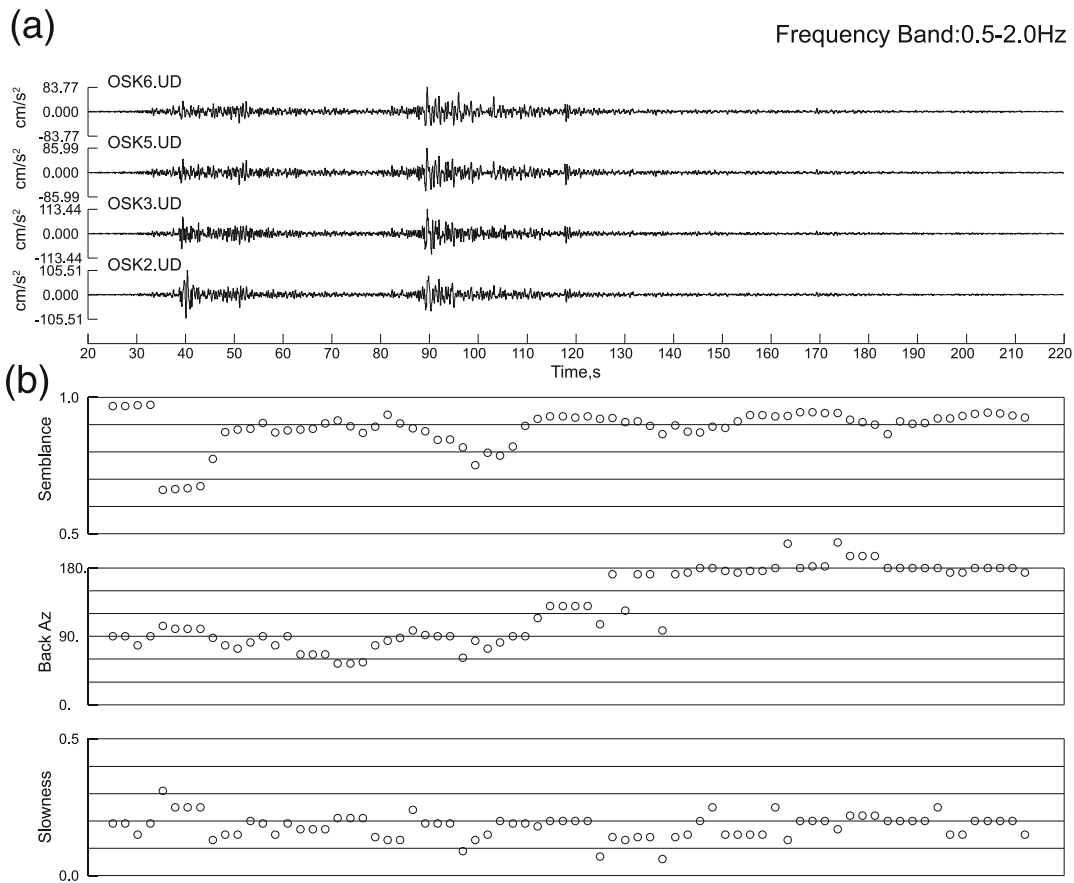


Fig. 3. Results of the semblance analysis. (a) UD-component acceleration records in the 0.5–2 Hz band are shown. (b) Semblance, back-azimuth, and horizontal slowness are shown from top to bottom.

results relating to the rupture propagation do not change so much. We set a time window of 10.24 s for the calculation of semblance in order to obtain a global image of the rupture propagation. At each station, a starting time of the window is adjusted according to a time shift expected for a plane wave propagating over the array with a given back-azimuth and slowness. We look for a back-azimuth and a slowness which maximize semblance by changing them in steps of 1° and 0.01 s/km, respectively. Sliding the time window by 2.56 s, we repeat the calculation. Though travel times should be corrected for differences in the subsurface structure and topography of each station in the array, we do not include such corrections in this analysis. This is because these corrections have not been estimated, but, even so, the back-azimuths of the *P*-wave and *S*-wave onsets are almost matched by the direction to the epicenter determined by JMA.

We use only the UD component for the semblance analysis, because the horizontal components were clearly clipped and probably distorted. Acceleration records of 200 s long are shown in Fig. 3(a). A direct *S*-wave from the hypocenter arrives at a time of 30 s. The obtained semblance values are higher than 0.8 for most of the waveforms as shown in the top panel of Fig. 3(b), suggesting that the observed phases are coherent. At times around 40 s, the semblance value decreases to 0.66. This is because the waveform at OSK2 might be clipped and distorted at this time. However, the semblance value of 0.66 is still high enough to accept.

In Fig. 1(a), back-azimuths from the array are drawn on the map. The back-azimuth for the *S*-wave onset at times of around 30 s is estimated to be about 80° . On the other hand, the back-azimuth of the epicenter determined by JMA is 99° . Therefore, our estimation of back-azimuths may have a bias error of about 20° maximum.

After the *S*-wave onset, back-azimuths remain at about 90° – 105° for about 10 s and decrease to 54° in the following 40 s. This suggests that the rupture mainly propagated in a northerly direction forming the first burst. During the second burst, which occurs at times of about 90–120 s, back-azimuths almost range from 90° – 130° indicating that the rupture moved to the southwest. Back-azimuths are about 170° and 190° for the other smaller bursts at times of about 140 s and 170 s, respectively, indicating that the rupture extended southwards.

The bottom panel of Fig. 3(b) shows the estimated horizontal slowness. Most of the slownesses are estimated to be 0.1–0.2 s/km. This suggests that the phases we analyzed consist of body waves, rather than surface waves which should be represented as much larger slowness. The slowness can be used to discriminate the depth of a location where the corresponding phase is emitted. For that purpose, we need to assume a seismic velocity structure and to identify incident phases to be *P*- or *S*-waves carefully. Because this paper aims to quickly report preliminary results on the rupture propagation, we only use back-azimuths as shown in Section 4.2 without assuming a seismic velocity struc-

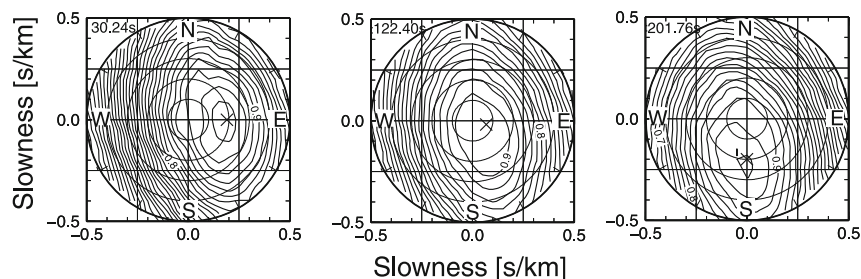


Fig. 4. Snapshots of semblance in slowness space. The results for three time windows centered at 30.24 s, 122.40 s and 201.76 s are shown from left to right. Semblance values are represented by contours with an interval of 0.02. Crosses show the location of the highest semblance value. N, S, E, and W indicate north, south, east and west directions.

ture.

In Fig. 4, we show semblance values in slowness space for three time windows centered at 30.24 s, 122.40 s and 201.76 s. The shape of the contours are like ellipses elongated slightly in the north-south direction. This is because the linear dimension of the array is slightly smaller in the north-south direction. We note that the location of the maximum semblance changes with time. The semblance contours are as expected for a single phase arrival, even for later time intervals, suggesting that the main energy arrives from one direction.

4. Discussions

4.1 Analysis of the March 9 earthquake

We also recorded strong ground motions from the March 9 earthquake (M_j 7.3), whose hypocenter was located by JMA to be 38.328°N , 143.280°E , at a depth of 8.3 km. The epicenter (a gray star in Fig. 1(a)) is situated about 45 km to the northeast of that of the Tohoku-Oki earthquake. This earthquake might be a foreshock. We similarly estimate the rupture propagation of the March 9 earthquake by applying the semblance technique. The analysis of this event also plays an important role to provide a calibration of the array for local seismic velocity structure. Figure 5(a) shows UD-component acceleration records in the 0.5–2 Hz band. It is notable that the amplitude is smaller by more than one order of magnitude than the Tohoku-Oki earthquake. The P -wave onset is found at about 15 s, and the S -wave onset at about 35 s in the figure. According to Fig. 5(b), back-azimuths are estimated to be about 80° at the both onsets. This value almost corresponds to 87° of the epicenter. We also note a difference in horizontal slowness between 0.14 s/km at the P -wave onset and 0.23 s/km at the S -wave onset. During larger amplitude motions between 35–50 s, back-azimuths stay between 55° and 80° . This suggests that the phases come from the fault. But after that, the back-azimuth starts to vary so much that they are out of range on the plot: Back-azimuths at times of 75–85 s become 340° – 350° suggesting that the phases are incident on the array from the northwest. These phases are probably scattered from heterogeneities in the Earth. On the other hand, it is remarkable that such a large variation in the back-azimuth is not found for the Tohoku-Oki earthquake as shown in Fig. 3. Therefore, it is reasonable to suppose that the observed phases come directly from the fault planes, and that we correctly observe rupture propagation during the Tohoku-Oki earthquake.

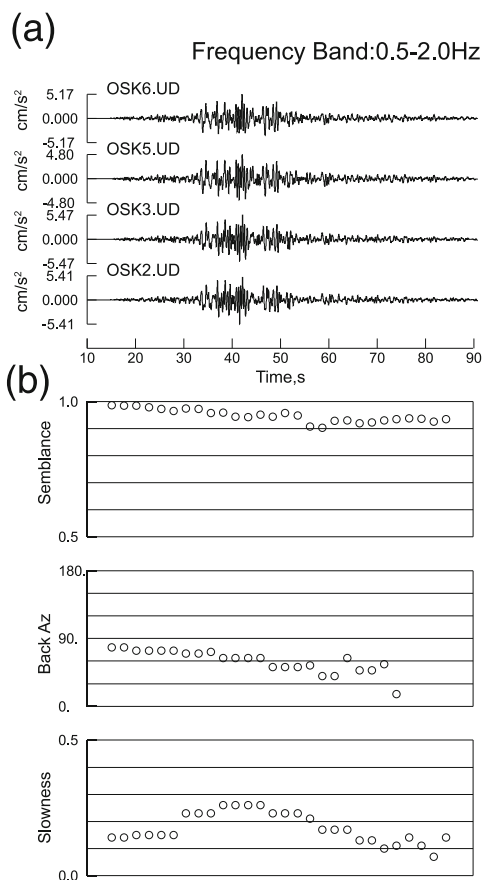


Fig. 5. Results of the semblance analysis for the March 9 earthquake. Time scale is the same as Fig. 3. The time of 0 s on the records is 11:45:24 on March 9, 2011 (JST). (a) UD-component acceleration records in the 0.5–2 Hz band are shown. (b) Semblance, back-azimuth, and horizontal slowness are shown from top to bottom.

4.2 Rupture propagation along the fault strike

Here, we investigate the rupture propagation for the Tohoku-Oki earthquake by projecting the incident phases back to a linear fault shown in Fig. 1(a) using only the back-azimuths estimated from the semblance analysis. The linear fault is assumed to be along a strike of 202° , the same as the northern subfault shown in Fig. 1(a), and is located on the surface at the halfway point with respect to the fault width. We measure a distance along the linear fault from the reference point where the linear fault intersects a line connecting the Oshika array with the epicenter. We convert the back-

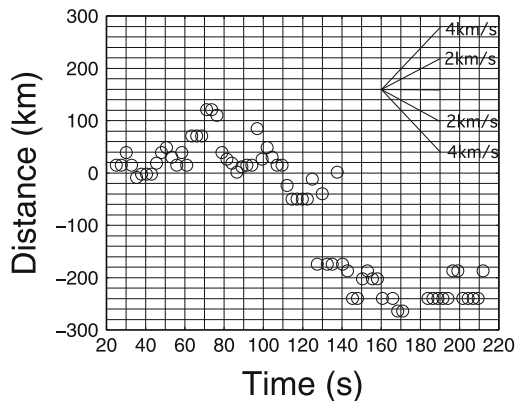


Fig. 6. Rupture propagation along the fault strike obtained from the projection to the linear fault. The horizontal axis is time, the same axis as Fig. 3. The vertical axis is the distance along the linear fault. Positive and negative distances correspond to the northeast and the southwest from the reference near the epicenter, respectively. A slope on the plot is proportional to the rupture velocity. For reference, 2 km/s and 4 km/s are shown by thick lines.

azimuth, which is measured every 2.56 s, to the distance, then plot the distance against time in Fig. 6.

The results suggest that the rupture during the Tohoku-Oki earthquake consists of at least four stages. The rupture propagated about 100 km in a northerly directions during times between 30 s and 80 s and apparently accelerated at times between 60 s and 80 s. The rupture seems to have restarted near the origin between 80 s and 100 s, then decreased to -60 km in the next 30 s. This indicates that the rupture propagated to the southwest off the Miyagi Prefecture. Then, the rupture suddenly jumped to the farther southwest at a time of 130 s. This jump implies that the rupture took place off the southern Fukushima Prefecture. And the rupture further extended to off Ibaraki Prefecture at times between 130 s and 170 s. The rupture seems to have mostly stayed at about -240 km at times between 180 s and 210 s.

We are reminded that additional information is necessary to discuss the rupture propagation perpendicular to the fault strike due to the linear projection. Acknowledging this restriction, we here make interpretations especially about the first and last stages of the rupture. Concerning the first stage, we cannot rule out the possibility that the rupture propagated in the north or northeast directions. However, the results can also be explained by the rupture propagating to the northwest off the Miyagi prefecture. We prefer this interpretation because the apparent rupture acceleration seen at 60–80 s can be naturally understood by the rupture propagating in the northwest direction with an almost constant velocity as a result of the projection. We also point out that the northeastward rupture might not have generated strong ground motions as exemplified in the previous subsection by notably smaller amplitudes for the March 9 earthquake. As for the last stage, the negligible change of back-azimuths around -240 km is unlikely to be the arrest of the rupture, because high-frequency waves were still observed for about 30 s. This apparent pause of the rupture can be understood by rupture propagation further to the south, parallel to the projection direction.

5. Conclusions

The Oshika array recorded strong ground motions from the Tohoku-Oki earthquake, and the data has enabled us to track the rupture propagation during the earthquake by semblance analysis. According to the results, the rupture during the Tohoku-Oki earthquake is considered to consist of at least four stages. Rupture propagated in northerly directions from the epicenter in the beginning 50 s forming the first burst, then proceeded to the southwest from around the epicenter in the next 50 s during the second burst. The rupture extended further southwestward in the following 40 s, and finally migrated further south for about 30 s. Because no assumptions have been made regarding the earthquake source process, this is a direct observation of rupture propagation during the earthquake. This study has demonstrated that a small seismic array enables the observation of rupture propagation during a large earthquake even with a small number of stations.

Acknowledgments. We are very grateful to Mr. Tokushichi Ito and Mr. Keiki Kuchiki for providing us with part of their pasture for our seismic array observation. Part of this observation was supported by the global COE program “Global Education and Research Center for Earth and Planetary Dynamics” of Tohoku University. We thank the research center for the prediction of earthquakes and volcanic eruptions, Tohoku University, for supporting data retrieval after the Tohoku-Oki earthquake. We appreciate the continuous encouragement of Prof. Shigeo Kinoshita, Yokohama City University, since the beginning of our observation. We thank an editor Prof. Kiyoshi Yomogida and Prof. Frederik Tilmann and an anonymous reviewer for constructive comments. We used the unified event catalogue compiled by the Japan Meteorological Agency and the Ministry of Education, Culture, Sports, Science and Technology in Japan. The GMT software (Wessel and Smith, 1998) and the SAC software (Goldstein *et al.*, 2003) were used for making the figures. We would like to offer our deepest condolences to the victims of the earthquake and tsunami.

References

- Editorial Committee of the Geologic Atlas of Japan, *Geologic Atlas of Japan—Tohoku Region*, Asakura Shoten, Tokyo, 1992.
- Geospatial Information Authority of Japan, Crustal Deformation and Fault Model obtained from GEONET data analysis, (web address: <http://www.gsi.go.jp/cais/topic110313-index-e.html>), 2011.
- Goldstein, P. and R. Archuleta, Deterministic frequency-wavenumber methods and direct measurements of rupture propagation during earthquakes using a dense array: Data analysis, *J. Geophys. Res.*, **96**, 6187–6198, 1991.
- Goldstein, P., D. Dodge, M. Firpo, and L. Minner, SAC2000: Signal processing and analysis tools for seismologists and engineers, invited contribution to “*The IASPEI International Handbook of Earthquake and Engineering Seismology*”, edited by W. H. K. Lee, H. Kanamori, P. C. Jennings, and C. Kisslinger, Academic Press, London, 2003.
- Honda, R., S. Aoi, H. Sekiguchi, and H. Fujiwara, Imaging an asperity of the 2003 Tokachi-oki earthquake using a dense strong-motion seismograph network, *Geophys. J. Int.*, **172**, 1104–1116, 2008.
- Ishii, M., P. M. Shearer, H. Houston, and J. E. Vidale, Extent, duration and speed of the 2004 Sumatra-Andaman earthquake imaged by the Hi-Net array, *Nature*, **435**, 933–936, 2005.
- Madariaga, R., High-frequency radiation from crack (stress drop) models of earthquake faulting, *Geophys. J. R. Astron. Soc.*, **51**, 625–651, 1977.
- Nakahara, H., K. Sawazaki, N. Takagi, T. Nishimura, H. Sato, and H. Fujiwara, Strong ground motions recorded by a near-source seismographic array during the 16 August 2005 Miyagi-Ken-Oki, JAPAN, earthquake (Mw 7.2), *Earth Planets Space*, **58**, 1555–1559, 2006.
- Neidell, N. S. and M. T. Taner, Semblance and other coherency measures for multichannel data, *Geophysics*, **36**, 482–497, 1971.
- Spudich, P. and E. Cranswick, Direct observation of rupture propagation

- during the 1979 Imperial Valley, California, earthquake using a short baseline accelerometer array, *Bull. Seismol. Soc. Am.*, **74**, 2083–2114, 1984.
- The Headquarters for Earthquake Research Promotion, List of long-term evaluation, (web address: <http://www.jishin.go.jp/main/choukihyoka/kaikou.htm>), 2005 (in Japanese).
- Wessel, P. and W. H. F. Smith, New improved version of the Generic Mapping Tools released, *Eos Trans. AGU*, **79**, 579, 1998.
-
- H. Nakahara (e-mail: naka@zisin.gp.tohoku.ac.jp), H. Sato, T. Nishimura, and H. Fujiwara